EVOLUTION & DEVELOPMENT 12:6, 568–579 (2010)
DOI: 10.1111/j.1525-142X.2010.00442.x

The *Gavialis–Tomistoma* debate: the contribution of skull ontogenetic allometry and growth trajectories to the study of crocodylian relationships

Paolo Piras,[a,b,*] Paolo Colangelo,[c] Dean C. Adams,[d] Angela Buscalioni,[e] Jorge Cubo,[f] Tassos Kotsakis,[a,b] Carlo Meloro,[g] and Pasquale Raia[h,b]

[a]Dipartimento di Scienze Geologiche, Università Roma Tre, Largo San Leonardo Murialdo, 1, 00146 Roma, Italy
[b]Center for Evolutionary Ecology, Largo San Leonardo Murialdo, 1, 00146 Roma, Italy
[c]Dipartimento di Biologia e Biotecnologie "Charles Darwin," Università di Roma "La Sapienza", via Borelli 50, 00161 Roma, Italy
[d]Department of Ecology, Evolution, and Organismal Biology, Iowa State University, Ames, IA 50011, USA
[e]Unidad de Paleontología, Departamento de Biología, Facultad de Ciencias, Universidad Autónoma de Madrid, 28049 Madrid, Spain
[f]Université Pierre et Marie Curie-Paris 6, UMR CNRS 7193-iSTeP, Equipe Biomineralisations, 4 Pl Jussieu, BC 19, Paris 75005, France
[g]Hull York Medical School, The University of Hull, Cottingham Road, Hull HU6 7RX, UK
[h]Dipartimento di Scienze della Terra, Universita' degli Studi Federico II, L.go San Marcellino 10, 80138 Napoli, Italy
*Author for correspondence (email: ppiras@uniroma3.it)

SUMMARY The phylogenetic placement of *Tomistoma* and *Gavialis* crocodiles depends largely upon whether molecular or morphological data are utilized. Molecular analyses consider them as sister taxa, whereas morphological/paleontological analyses set *Gavialis* apart from *Tomistoma* and other crocodylian species. Here skull allometric trajectories of *Tomistoma* and *Gavialis* were contrasted with those of two longirostral crocodylian taxa, *Crocodylus acutus* and *Mecistops cataphractus*, to examine similarities in growth trajectories in light of this phylogenetic controversy. Entire skull shape and its two main modules, rostrum and postrostrum, were analyzed separately. We tested differences for both multivariate angles between trajectories and for shape differences at early and late stages of development. Based on a multivariate regression of shape data and size, *Tomistoma* seems to possess a peculiar rate of growth in comparison to the remaining taxa. However, its morphology at both juvenile and adult sizes is always closer to those of Brevirostres crocodylians, for the entire head shape, as well as the shape of the postrostrum and rostrum. By contrast, the allometric trajectory of *Gavialis* always begins and ends in a unique region of the multidimensional morphospace. These findings concur with a morphological hypothesis that places *Gavialis* separate from Brevirostres, and *Tomistoma* closer to other crocodylids, and provides an additional, and independent, data set to inform on this ongoing phylogenetic discussion.

INTRODUCTION

The phylogenetic relationships between the true-gharial (*Gavialis gangeticus*) and the false-gharial (*Tomistoma schlegelii*) continue to be discussed because the outcomes of molecular and morphological analyses are so contradictory. Specifically, analyses of various and distinct molecular data sets support a close evolutionary relationship between these two genera, with an Eocene or mid-Miocene divergence (Fig. 1A). Thus, from a molecular perspective, *Gavialis* and *Tomistoma* are each others' closest living relatives. By contrast, morphological data support the placement of *Gavialis* basal to Crocodylia, implying that *Gavials* and *Tomistoma* are morphologically similar longirostrine forms, that have evolved this morphology multiple times, and stratigraphic data imply that this split occurred by the Late Cretaceous (Fig. 1B). Both views are well supported by multiple recent studies (Brochu and Densmore 2001; Brochu 2003; Gatesy et al. 2003; Harshman et al. 2003; Janke et al. 2006; Xue-Feng et al. 2006; McAliley et al. 2006, among others), and because resolution across data types has not yet been found, the *Gavialis*/*Tomistoma* debate represents a classic phylogenetic conflict in the literature (Brochu 2003).

Typically, explanations for the discrepancy between these phylogenetic hypotheses are grounded on the nature of the phylogenetic methods applied and their potential limitations (i.e., rooting problems, long-branch attraction due to taxon-

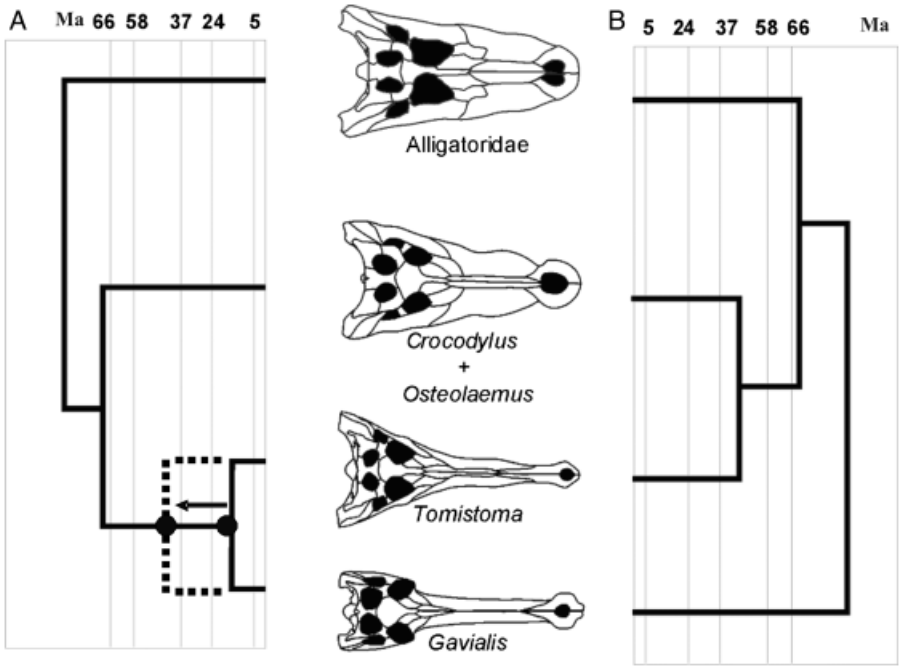

Fig. 1. Competing hypotheses about phylogenetic relationships for *Gavialis* and *Tomistoma*. (A) Molecular topology; dashed line indicates the oldest split proposed by a molecular study (Janke et al. 2006); (B) morphological/paleontological topology. From Brochu (2003), redrawn.

sampling, different phylogenetic histories between genes and species), as well as morphological or physiological convergence. For example, previous authors have investigated the differential contribution of phylogeny and functional performance on the biomechanical properties of rostrum in extant Crocodylia (Piras et al. 2009), and on the differences in rostral architecture in extant and extinct Crocodylomorpha (Busbey, 1995). However, a detailed study focusing on the ontogenetic development of the morphological differences between *Gavialis* and *Tomistoma* has not been performed. Here we analyzed and compared ontogenetic trajectories of several species in order to bring new evidence to the *Tomistoma–Gavialis* phylogeny debate. Studies of ontogenetic variation quantify aspects of morphogenetic change during growth. In interspecific comparisons, early ontogenetic stages may or may be not closer to each other than adult stages (Zelditch et al. 2004). For example, if shapes become more and more similar during growth, then morphological resemblance of adult forms may be the outcome of evolutionary convergence or parallelism. In such cases, phylogenetic reconstructions based on adult morphology alone may not accurately estimate evolutionary history, because it does not include the allometric processes responsible of the final product of ontogenesis, that is adult phenotypes, without taking into account common factors in development between species. Conversely, increasingly divergent ontogenies may indicate that the adult forms appear very different in spite of small phylogenetic distance as an outcome of morphological adaptation.

We used an ontogenetic approach to determine whether *Gavialis* and *Tomistoma* displayed convergent growth patterns (ontogenetic convergence: sensu Adams and Nistri 2010). We explored the pattern of shape variation along the ontogeny of both *Tomistoma* and *Gavialis*, as well as two other species of Crocodylia (*Crocodylus acutus* and *Mecistops cataphractus*). The latter two species are of interest because they possess a long snout (i.e., longirostral), and our samples cover nearly all posthatching ontogenetic stages; allowing a rigorous assessment of the ontogenetic development of this trait. Of the species we examined, only *Gavialis* "gharial" is a strictly piscivorous species, while the other three species can consume prey that are relatively larger than fishes, despite their longirostral condition. The rationale for using *M. cataphractus* and *C. acutus* is both their phylogenetic placement, and the fact that they represent morphological extremes. Specifically, *M. cataphractus* displays the least derived morphology of species of Crocodylinae, and *C. acutus* is one of the most longirostral species within *Crocodylus*.

We used landmark-based Geometric Morphometrics (GM) to analyze phenotypic differences and ontogenetic trajectories covering all the long-snouted genera of crocodylians. First, we analyzed the complete skull geometry found from all landmarks, to investigate general patterns on skull ontogeny. Second, we partitioned the landmark data set was into two units (the rostrum and the postrostrum), which were analyzed separately. Using these three data sets we tested a number of specific biological hypotheses with respect to size and shape variation in these species. First, we tested the hypothesis that different species possess similar allometry by analyzing differences in multivariate slopes. Second we determined whether the ontogenetic trajectories for species are parallel, convergent, or divergent in

the multidimensional morphogenetic space. If *Tomistoma* was phylogenetically related to Crocodylidae, we predicted that there would be strong similarities between its ontogenetic growth pattern and those of other members of that clade.

MATERIAL AND METHODS

GM

A total of 93 skull specimens spanning nearly all posthatching sizes of *T. schlegelii* ($n = 17$), *M. cataphractus* ($n = 24$), *C. acutus* ($n = 32$), and *G. gangeticus* ($n = 20$) were analyzed (see supporting information Appendix S1). Only complete skulls of individuals captured in the wild and lacking evident bone abnormalities were included. We used landmark-based GM methods to quantify overall skull shape (Bookstein 1991; Rohlf and Marcus 1993; Adams et al. 2004; Zelditch et al. 2004; Mitteroecker and Gunz 2009). These methods quantify the shape of anatomical objects from the coordinates of repeatable locations, after the effects of nonshape variation are mathematically held constant. For each specimen, 90 3-dimensional landmarks were digitized (using an Immersion Microscribe G2) from the left side of the skull to capture skull geometry. Landmark definitions, positions and their corresponding configurations are shown in Fig. 2. This landmark configuration was then divided into two parts assumed to behave as separate developmental modules: a "rostral" module and a "postrostral" module (Brochu, 2001). Twenty-one landmarks defined the rostrum and 41 landmarks defined the postrostrum. We aligned the set of landmark coordinates using a generalized Procrustes Analysis (GPA), which superimposes specimens to a common coordinate system after accounting for differences in position, orientation, and scale (Rohlf and Slice 1990; Bookstein 1991; Goodall 1991). From the aligned specimens, Procrustes shape coordinates were obtained, and used as shape variables in subsequent statistical analyses (e.g., Bookstein 1986; Mitteroecker et al. 2004; Mitteroecker and Bookstein 2008). Centroid size was also retained for subsequent allometric analyses. A separate GPA was performed on the entire data set, as well as on each developmental module.

Comparing ontogenetic allometry

To test the hypothesis that species differ in their allometric trajectories, we used permutational MANCOVA, with species, size,

Fig. 2. Landmark positions on the *Tomistoma schlegelii* skull and relative configurations. (A) Ventral view. (B) Dorsal view. (C) Lateral view. (D) Occipital view. (E) Neurocranial landmarks. (F) Prefrontal pillar detail. (G) Entire shape configuration. (H) Postrostral configuration. (I) Rostral configuration. Landmark definitions: 1: Anterior tip of anterior lateral projection of squamosal-postorbital suture; 2: Triple joint between maxilla, jugal, and ectopterygoid; 3: Dorsal contact between ectopterygoid-pterygoid in lateral aspect; 4: Ventral tip of foramen ovale; 5: Antero-dorsal laterosphenoid projection at its contact with the frontal; 6: Emergence of the basisphenoid rostrum, caudal point; 7: Ventro-lateral edge of II cranial nerve emergence; 8: Dorso-lateral projection of laterosphenoid; 9: Dorsal palatine projection on prefrontal pillar; 10: Ventral tip of the pterygoid wing; 11: Posterior angle of infratemporal fenestra; 12: Anterior angle of infratemporal fenestra (on the posterior surface of postorbital bar); 13: Dorsal angle of infratemporal fenestra; *Landmarks in dorsal aspect*: 14: Medial dorsal anterior projection of frontal; 15: Medial dorsal anterior projection of nasal; 16: Postero-lateral tip of external nares opening; 17: Anterior tip of external nares opening (in *Alligator* and *Osteolaemus* this simply corresponds to its anterior profile); 18: Postero-lateral tip of premaxilla; 19: On dorsal skull roof, lateral edge of squamosal-postorbital contact; 20: Triple joint between nasal, prefrontal, and lachrymal; 21: Triple joint between maxilla, jugal, and lachrymal; 22: Postero-lateral orbital tip (on jugal border just anterior to postorbital bar); 23: Triple joint between frontal, parietal, and postorbital; 24: Triple joint between frontal, prefrontal, and nasals; 25: Entrance of prefronto-lachrymal suture at the orbit; 26: Entrance of squamoso-postorbital suture at the supratemporal fenestra; 27: Triple joint between nasals, maxilla, and lachrymal (if this latter contacts); 28: Entrance of parietal-squamosal suture in supratemporal fenestra; 29: Anterior medial contact between parietal and supraoccipital; 30: Posterior edge of skull roof just at squamosal postero-medial border; 31: Entrance of jugolachrymal suture at the orbit; 32: Entrance of frontopostorbital suture at the orbit; 33: Entrance of fronto-prefrontal suture at the orbit; 34: Entrance of fronto-postorbital suture at the supratemporal fenestra; 35: Anterior tip of the orbital contour; 36: Distal tip of the premaxilla; 37: Postero-lateral squamosal projection on the skull roof; 38: Distal tip of the external nares contour; 39: Anterior tip of the premaxilla; 40: Posterior tip of the supraoccipital; 41: Posterior medial tip of the skull roof; 42: Maximum skull width; 43: Antero-lateral postorbital tip on skull roof; 44: Antero-orbital lateral-most skull edge; 45: Lateral-most edge of the skull posterior to postorbital bar; 46: Anterior tip of supratemporal fenestra; 47: Medial tip of supratemporal fenestra; *Landmarks in ventral aspect*: 48: Posterior-most ventral tip of maxillo-premaxillary contact; 49: Anterior-most tip of maxillo-palatine contact; 50: Anterior-most edge of the palatine fenestra; 51: Anterior tip of ectopterygoid-maxillary contact; 52: Entrance of the palatino-pterygoid suture at the palatine fenestra; 53: Entrance of ectopterygoid-pterygoid suture at the palatine fenestra; 54: Premaxillary constriction solely on premaxillo-maxillary suture, along the alveolar margin; 55: Posterior ventral projection of jugal-quadratojugal suture; 56: Posterior projection of quadratojugal and quadrate suture; 57: Lateral tip of 4th alveolus; 58: Lateral tip of 5th alveolus; 59: Medial tip of 5th alveolus; 60: Medial tip of 4th alveolus; 61: Lateral tip of 7th alveolus; 62: Lateral tip of 8th alveolus; 63: Lateral tip of 11th alveolus; 64: Lateral tip of 12th alveolus; 65: Anterior tip of the choana; 66: Posterior tip of the choana; 67: Lateral tip of the choana; 68: Anterior tip of the incisive foramen; 69: Lateral tip of the palatine fenestra; 70: Medial edge of palatine fenestra; 71: Posterior tip of the palatine fenestra; *Landmarks in occipital aspect*: 72: Triple joint between supraoccipital, squamosal, and exoccipital; 73: Dorsal tip of the foramen magnum; 74: Mid-joint between supraoccipital and exoccipitals; 75: Ventro-lateral projection of paraoccipital process; 76: Lateral tip of basioccipital just at exoccipital-basioccipital suture; 77: Ventro-medial contact between pterygoid and basisphenoid; 78: Ventral tip of the foramen magnum; 79: Lateral tip of the foramen magnum; 80: Dorso-lateral projection of the paraoccipital process; 81: Ventro-lateral tip of the basioccipital tubera; 82: Postero-lateral tip of the pterygoid posterior process; 83: Dorso-lateral tip of medial quadrate hemicondyle; 84: Ventro-lateral tip of medial quadrate hemicondyle; 85: Dorso-lateral tip of distal quadrate hemicondyle; 86: Ventro-lateral tip of distal quadrate hemicondyle; 87: Lateral tip of the basioccipital condyle; 88: Dorsal tip of the basioccipital condyle; 89: Ventral tip of the basioccipital condyle; 90: Posterior tip of the supratemporal fenestra. Rostral configuration was obtained with the following landmarks: 14–18, 35–36, 38–39, 48–49, 54, 57–64, 68. Postrostral configuration was obtained with the following landmarks: 1, 10–14, 19–20, 22, 24–28, 31–34,37, 40–47, 50, 69–71, 73, 75–79, 83, 85, 89–90.

and species × size as factors. Permutational MANCOVA is based on the Euclidean (Procrustes) distances among individuals, and was used because the number of shape variables greatly exceeded the number of specimens. The statistical significance of terms in the model was determined using 10,000 permutations (for details see Anderson 2001). Subsequent to this analysis, differences between pairs of allometric trajectories were assessed using a modification of phenotypic trajectory analysis (Collyer and Adams 2007; Adams and Collyer 2007; Adams and Collyer 2009). Here, the observed allometric trajectory for each species was estimated by the set of regression coefficients of a regression of shape on size. Because the number of shape variables exceeded the number of specimens, we performed a principal component analysis of shape, and retained only those dimensions that contained variation. Differences between trajectories were then calculated as the Euclidean distance between vectors of slopes, disregarding the intercept. Regression vectors without the intercept are "centered" at the origin; thus, distances between vectors of slopes are equivalent to the angle between their multivariate regression lines. Next, residuals from a reduced model containing only species and size (without the interaction term) were obtained, and were permuted among species. Regression coefficients from the randomized data were then obtained, and differences between randomized allometric trajectories were estimated. The observed differences between allometric trajectories were then compared with a randomly generated distribution of trajectories, consisting of 999 iterations obtained by permuting the residuals as above. Given that six pairwise comparisons were made, significance level was set to an experiment-wise error rate of $\alpha = 0.05$, using Bonferroni's correction ($\alpha_{pairwise} = 0.05/6 = 0.0083$).

In order to explore shape differences at the onset of posthatching growth we calculated predicted shapes for each species at the smallest comparable sizes recorded for any species. We then calculated the observed Euclidean (Procrustes) distances between them, and compared this to a distribution of random distances, using the permutation procedure described above. Finally, in order to graphically assess the similarities in multivariate growth trajectories and in early posthatching stage differences, we generated UPGMA dendrograms based on distances between multivariate angles and between predicted shapes at smallest and largest comparable sizes.

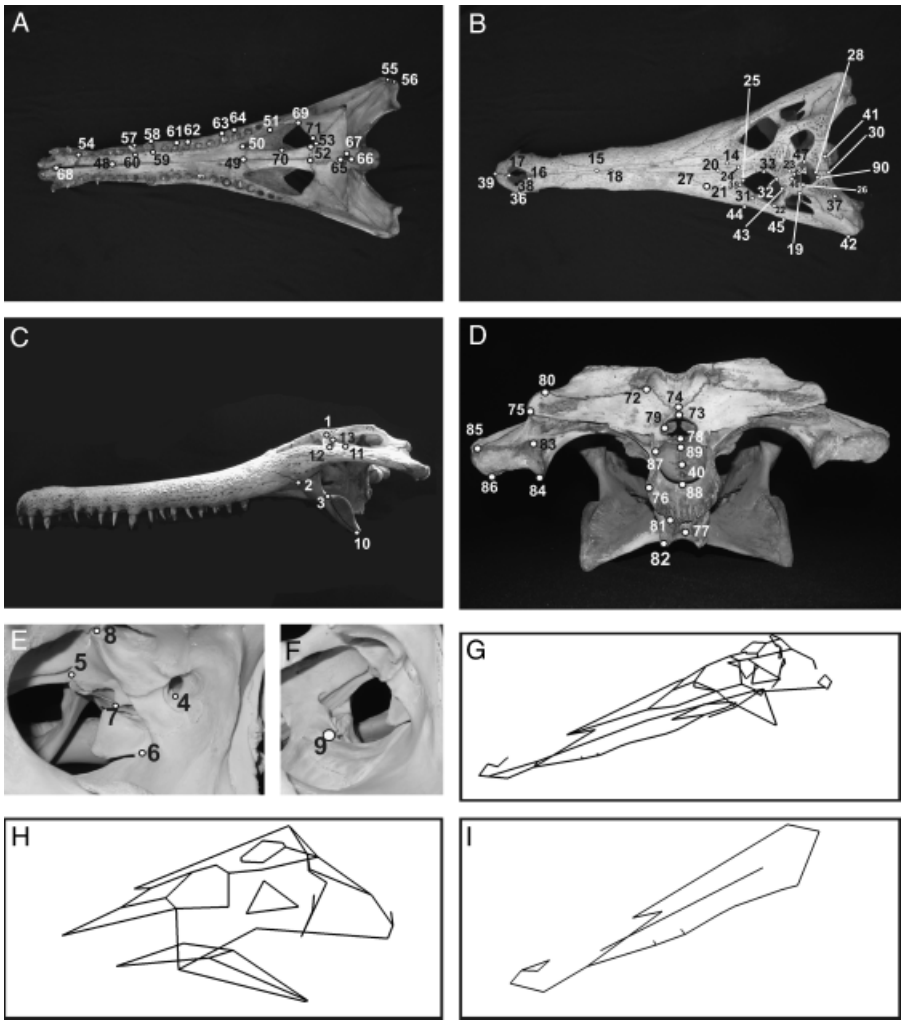

Table 1. Multivariate angular distances between ontogenetic trajectories of species

		Angles			
Entire shape		*Ca*	*Mcat*	*Gg*	*Ts*
	Ca	0.000			
	Mcat	0.055	0.000		
	Gg	0.102	0.067	0.000	
	Ts	0.157	0.120	0.106	0.000
	P-value				
		Ca	*Mcat*	*Gg*	*Ts*
	Ca	1.000			
	Mcat	0.021	1.000		
	Gg	**0.001**	0.013	1.000	
	Ts	**0.003**	0.014	0.035	1.000
		Angles			
Postrostrum		*Ca*	*Mcat*	*Gg*	*Ts*
	Ca	0.000			
	Mcat	0.048	0.000		
	Gg	0.117	0.107	0.000	
	Ts	0.111	0.094	0.094	0.000
	P-value				
		Ca	*Mcat*	*Gg*	*Ts*
	Ca	1.000			
	Mcat	0.230	1.000		
	Gg	**0.001**	**0.001**	1.000	
	Ts	0.021	0.105	0.097	1.000
		Angles			
Rostrum		*Ca*	*Mcat*	*Gg*	*Ts*
	Ca	0.000			
	Mcat	0.058	0.000		
	Gg	0.115	0.079	0.000	
	Ts	0.189	0.152	0.166	0.000
	P-value				
		Ca	*Mcat*	*Gg*	*Ts*
	Ca	1			
	Mcat	0.085	1		
	Gg	**0.001**	0.028	1	
	Ts	0.013	0.03	0.022	1

Significance based on 1000 randomizations. In bold significant differences. Significance level was set at 0.008, following Bonferroni's adjustment.

Testing for convergence and parallelism

To determine whether developmental trajectories were convergent, parallel, or divergent we followed the procedure of Adams and Nistri (2010). First, we quantified the Procrustes distances between predicted shapes among species at both the smallest and largest comparable size values. We then calculate pairwise distances between species at both small and large sizes and contrasted them. If the morphological distance between two species is significantly smaller at adult stages as compared with at juvenile stages, this pattern provides evidence for ontogenetic convergence; if distance remains the same (i.e., the difference was not statistically significant) there is evidence for parallelism, and if the distance between species is significantly larger in adults than in juveniles there is evidence for divergence. We statistically assessed these patterns using a permutation procedure (with 9999 randomizations), where the Procrustes shape coordinates for individuals were shuffled with respect to size, and the differences in Procrustes distances between simulated datasets of large and small individuals among species were recalculated and compared with the observed values (for a related approach for assessing parallel evolution see Adams 2010).

Visualizing ontogenetic allometry

The visualization of phenotypic growth trajectories from GM data is challenging, because shape data are highly multivariate. We used several approaches to visualize allometric trends. First, we used principal components analysis to examine patterns of variation using the set of Procrustes shape variables. We visualized shape variation along the first three principal component axes. Additionally, we included size in this plot, by scaling each point proportional to the centroid size of each specimen. This allowed us to incorporate allometry into the visualization. Second, we visualized allometric trajectories using predicted shapes along the regression curve (Mitteroecker and Bookstein 2005). Here, separate linear regressions of shape on size ($\log_{10}$CS) are performed for each

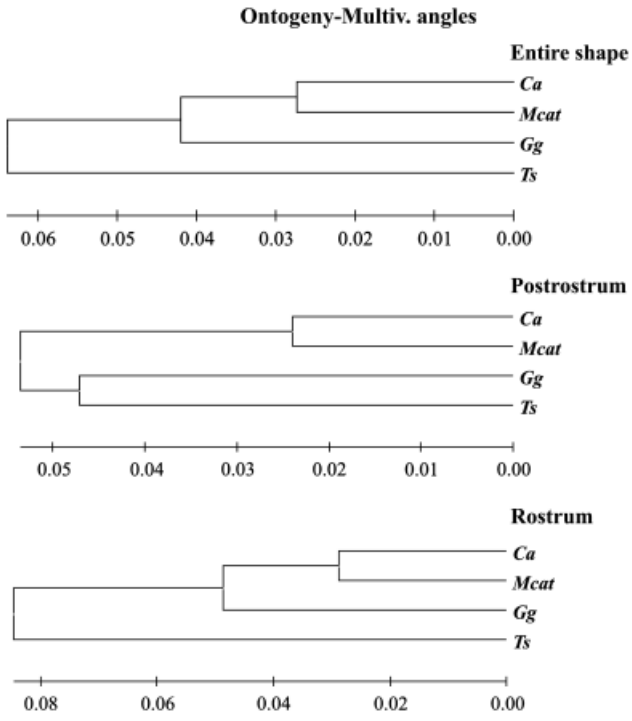

Fig. 3. UPGMA clusters generated from pairwise angular similarities in the direction of ontogenetic trajectories in morphospace. *Ca*, *Crocodylus acutus*; *Mcat*, *Mecistops cataphractus*; *Gg*, *Gavialis gangeticus*; *Ts*, *Tomistoma schlegelii*.

Table 2. Species-specific patterns of covariation between shape and size

Entire shape		
	% variance explained after Regression	
Ca	0.42 (simulated *P*-value: <0.001)	
Mc	0.26 (simulated *P*-value: <0.001)	
Gg	0.51 (simulated *P*-value: <0.001)	
Ts	0.41 (simulated *P*-value: <0.001)	
Postrostrum		Regression with entire shape size
	% variance explained after Regression	% variance explained after Regression
Ca	0.50 (simulated *P*-value: <0.001)	0.49 (simulated *P*-value: <0.001)
Mc	0.36 (simulated *P*-value: <0.001)	0.35 (simulated *P*-value: <0.001)
Gg	0.67 (simulated *P*-value: <0.001)	0.66 (simulated *P*-value: <0.001)
Ts	0.39 (simulated *P*-value: <0.001)	0.37 (simulated *P*-value: <0.001)
Rostrum		Regression with entire shape size
	% variance explained after Regression	% variance explained after Regression
Ca	0.36 (simulated *P*-value: <0.001)	0.36 (simulated *P*-value: <0.001)
Mc	0.15 (simulated *P*-value: <0.001)	0.15 (simulated *P*-value: <0.001)
Gg	0.19 (simulated *P*-value: <0.001)	0.20 (simulated *P*-value: <0.001)
Ts	0.31 (simulated *P*-value: <0.001)	0.37 (simulated *P*-value: <0.001)

Simulated *P*-values based on 1000 randomizations are given in parentheses.

species, and predicted values are obtained. We then summarized this variation by using principal components, and plotted variation along predicted allometric trajectories in the first three dimensions. As with patterns in Procrustes shape variables, each point in morphospace was scaled by its centroid size, allowing a visual assessment of allometry.

RESULTS

Ontogeny: entire shape, postrostrum, and rostrum

Using multivariate regression, patterns of shape allometry we found that *Tomistoma* has a different growth trajectory, relative to the other species. This is best seen in the differences of multivariate angles between species in their allometric trajectories (Table 1), and in the UPGMA dendrograms summarizing these relationships (Fig. 3). Further, Procrustes distances between small and large individuals for each species revealed that *Tomistoma* displayed a greater change in shape per unit size than did the remaining species. Therefore, this species attains a higher "rate of growth" in terms of shape change per unit size (not age). Individual analyses of species-specific multivariate allometry identified that *Gavialis* and *Mecistops* had the smallest covariation between rostrum shape and size, while *Tomistoma* had similar values as compared with *Crocodylus*. In addition, *Gavialis* had the largest degree of covariation between postrostrum shape and size (Table 2). Visualizing these ontogenetic trajectories (Fig. 4) shows that PCAs of predicted shapes clearly provides a better representation of the actual ontogenetic trajectories than just the amount of the original shapes that is explained by size change. Further, some species appear more similar in their multivariate allometric trajectories than do others. Finally, it appears that for some skull components, adults among species are more similar to one another than are juveniles (Fig. 4 and below).

Predicted shapes along allometry curves (Fig. 5) corresponded to juvenile and adult morphologies. Examining the shape of the entire skull, we found a relative reduction of orbits throughout the course of development for all taxa. When compared with the other taxa, the orbits of *Gavialis* become more telescopic during growth, and the pterygoidal flange remains closer to the quadrate lateral expansion. Additionally, the nasal bone never contacts the premaxilla in *Gavialis*. By contrast, in *Tomistoma*, *Crocodylus*, and *Mecistops*, there is a general widening of the maxilla during growth. In all species, the postrostrum module shows a common pattern of shape change, with a reduction of orbit dimensions and a widening of the "cranial nipper" formed by quadrate lateral expansion and the pterygoidal flange. Of these species, *Gavialis* displays the least widening of the "cranial nipper" during growth, and has the largest supratemporal and infratemporal fenestrae of all species.

Patterns of rostrum shape change show that *Gavialis* has a unique rostrum morphology: the widening of the maxilla is very reduced in comparison to *Tomistoma* or *Crocodylus*, and the 12th alveolus remains posteriorly shifted relative to the

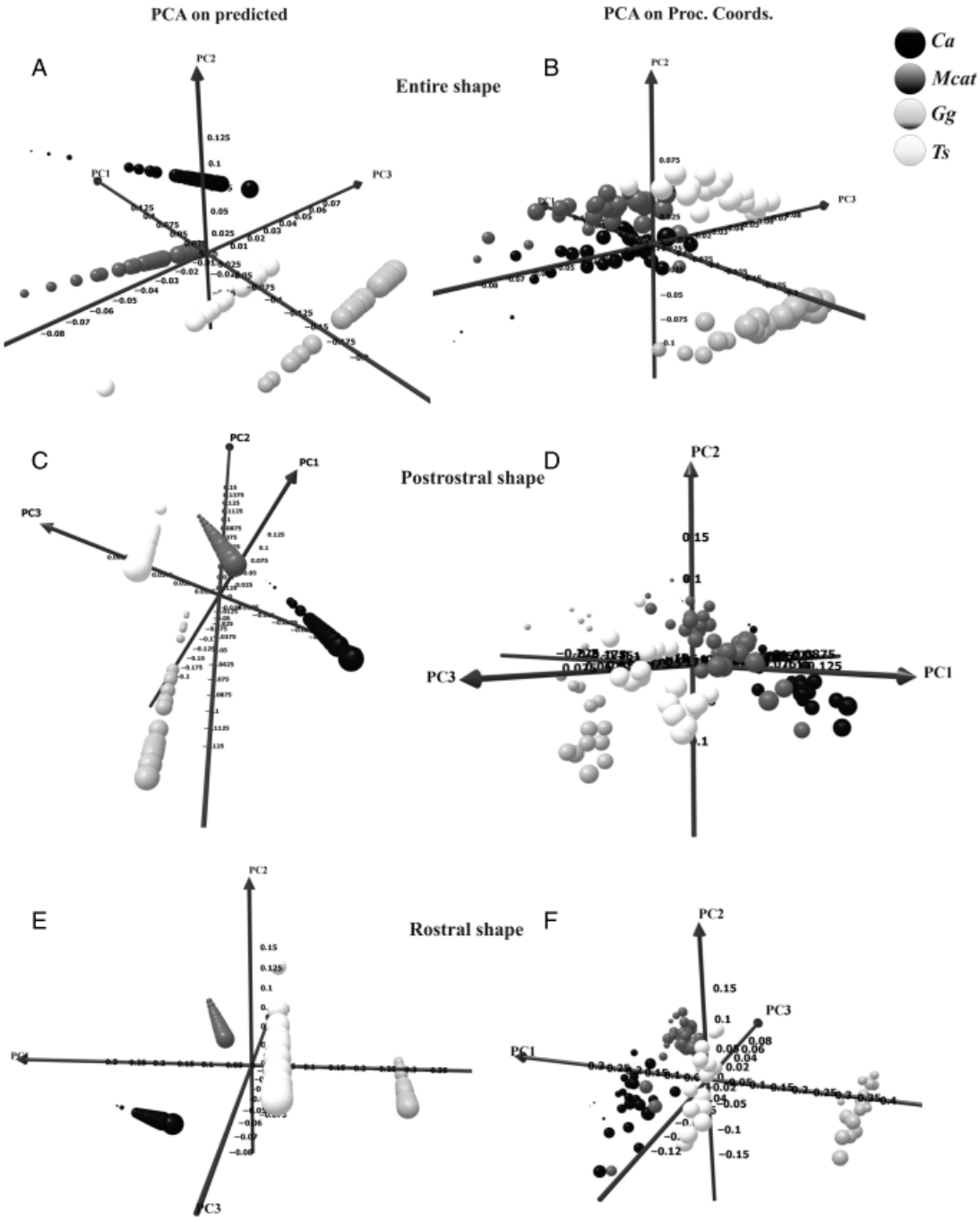

Fig. 4. Ontogenetic trajectories for each of the three morphological data sets (entire skull, postrostrum, and rostrum), computed from PCAs of predicted shapes, after species-specific linear regressions of shape on size (A, C, and E) and on Procrustes residuals (B, D, and F). Separate Procrustes fits have been performed for the three landmark data sets. The size of each symbol is proportional to the size of the specimen, indicating the direction of ontogenetic change (small → large). *Ca*, *Crocodylus acutus*; *Mcat*, *Mecistops cataphractus*; *Gg*, *Gavialis gangeticus*; *Ts*, *Tomistoma schlegelii*.

anterior tip of frontal spine during growth. On the other hand, *Crocodyus* and *Mecistops* are similar to *Gavialis* in their juvenile morphologies, but display a converse pattern as adults, where the anterior tip of the frontal spine is posteriorly shifted relative to 12th alveolus position. *Tomistoma* is peculiar in this regard because the 12th alveolus is anteriorly shifted relative to the anterior tip of the frontal spine at both the juvenile and adult stages of development.

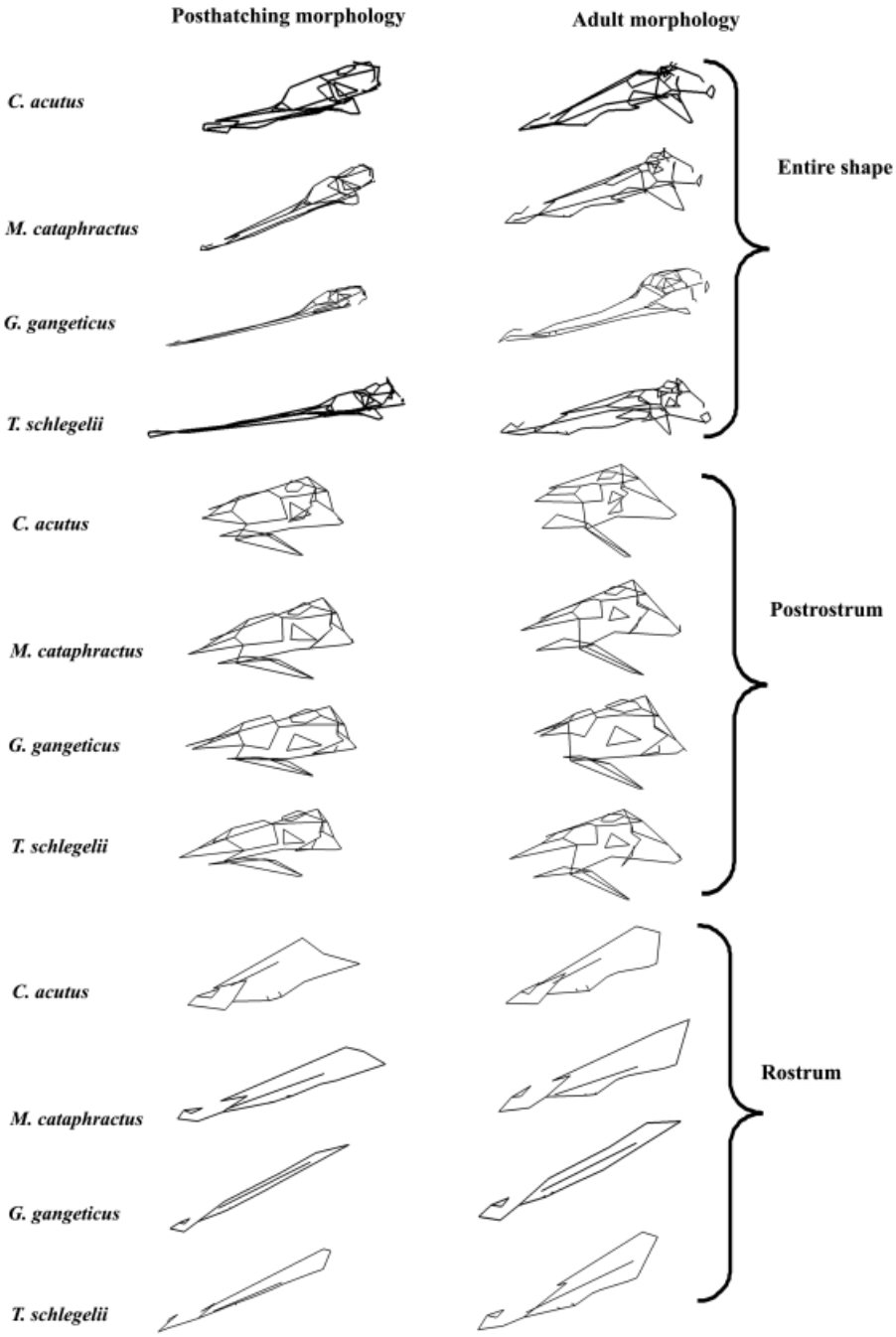

Fig. 5. Ontogenetic morphological changes visualized after species-specific multivariate regressions of shape on size for the three landmark data sets.

Test for ontogenetic convergence

Using multivariate ontogenetic trajectories, we observed significant convergence in entire shape between *Gavialis* and the other taxa, but not between *Tomistoma* and any of the other taxa (Table 3). Ontogenetic convergence was also present between *Crocodylus* and *Mecistops*. The remaining trajectories were not statistically different from one another, implying ontogenetic parallelism in their patterns of growth. The analysis of postrostral shape suggests divergence between *Gavialis* and all other taxa (Table 3), while the remaining species display parallelism in their ontogenetic trajectories. The exception to this is the *Mecistops* and *Crocodylus*, whose ontogenetic trajectories diverge in relatively different adult morphologies.

In terms of rostral shape, most species exhibit parallel trajectories. The exception to this was *Gavialis*, which is

Table 3. Tests for ontogenetic convergence

Entire shape					Postrostrum				Rostrum				
Differences between small and large Procrustes distance between species													
	Ca	*Mcat*	*Gg*	*Ts*		*Ca*	*Mcat*	*Gg*	*Ts*		*Ca*	*Mcat*	*Gg*	*Ts*
Ca	0.00000				*Ca*	0.00000				*Ca*	0.00000			
Mcat	0.00769	0.00000			*Mcat*	−0.01061	0.00000			*Mcat*	0.01196	0.00000		
Gg	0.03524	0.01502	0.00000		*Gg*	−0.05971	−0.04800	0.00000		*Gg*	0.03733	0.02196	0.00000	
Ts	0.07372	0.03911	0.00406	0.00000	*Ts*	0.00417	−0.00602	−0.02828	0.00000	*Ts*	0.03620	−0.00520	0.05436	0.00000
Procrustes distance at small sizes														
	Ca	*Mcat*	*Gg*	*Ts*		*Ca*	*Mcat*	*Gg*	*Ts*		*Ca*	*Mcat*	*Gg*	*Ts*
Ca	0.00000				*Ca*	0.00000				*Ca*	0.00000			
Mcat	0.09057	0.00000			*Mcat*	0.08988	0.00000			*Mcat*	0.13927	0.00000		
Gg	0.29033	0.23698	0.00000		*Gg*	0.18343	0.18787	0.00000		*Gg*	0.55243	0.46097	0.00000	
Ts	0.20471	0.13339	0.18050	0.00000	*Ts*	0.12897	0.09393	0.19273	0.00000	*Ts*	0.30683	0.18327	0.35697	0.00000
Procrustes distance at large sizes														
	Ca	*Mcat*	*Gg*	*Ts*		*Ca*	*Mcat*	*Gg*	*Ts*		*Ca*	*Mcat*	*Gg*	*Ts*
Ca	0.00000				*Ca*	0.00000				*Ca*	0.00000			
Mcat	0.08288	0.00000			*Mcat*	0.10048	0.00000			*Mcat*	0.12731	0.00000		
Gg	0.25508	0.22195	0.00000		*Gg*	0.24314	0.23587	0.00000		*Gg*	0.51510	0.43902	0.00000	
Ts	0.13099	0.09428	0.17644	0.00000	*Ts*	0.12481	0.09995	0.22101	0.00000	*Ts*	0.27062	0.18847	0.30261	0.00000
Simulated *P*-value for significance in differences after 10,000 permutations														
	Ca	*Mcat*	*Gg*	*Ts*		*Ca*	*Mcat*	*Gg*	*Ts*		*Ca*	*Mcat*	*Gg*	*Ts*
Ca	1.00000				*Ca*	1.00000				*Ca*	1.00000			
Mcat	**0.0014C**	1.00000			*Mcat*	**0.0025D**	1.00000			*Mcat*	0.0224P	1.00000		
Gg	**0.0001C**	**0.0001C**	1.00000		*Gg*	**0.0001D**	**0.0001D**	1.00000		*Gg*	**0.0001C**	**0.0001C**	1.00000	
Ts	0.0109P	0.1262P	0.0342P	1.00000	*Ts*	0.105P	0.3881P	**0.005D**	1.00000	*Ts*	0.0601P	0.2929P	0.0255P	1.00000

Significant differences in bold. Significance level was set at 0.008, based on Bonferroni's adjustment.
C, convergence; D, divergence; P, parallelism.

convergent with both *Crocodylus* and *Mecistops*. Dendrograms based on Procrustes distances between predicted shapes at comparable small and large sizes among species visually confirm these findings (Fig. 6). *Gavialis* is the most peculiar taxon in terms of skull shape, regardless of whether small or large individuals are examined. This pattern is congruent with the morphological phylogeny for the species, implying that at both the onset of posthatching growth and at late developmental stages, the morphology of *Gavialis* is quite distinct from that observed in the other taxa.

DISCUSSION

The difference between molecular and morphological crocodilian phylogenies, and the relative positions of *Gavialis* and *Tomistoma* in particular, have proven difficult to reconcile. Combined morphological-molecular analyses reiterate the "morphological" topology when fossil species are included, a pattern similarly observed in the molecular data, when they are limited to the 12S ribosome sequences (Brochu, 2003). However, when larger molecular data sets are used (e.g., Gatesy et al. 2003, 2004), phylogenetic patterns converge on an alternative topology (Brochu 2003). The differential signals between data types have also proven to be highly stable when new data or taxa are added. Here we addressed this puzzling issue from a completely different perspective, examining the signal in ontogenetic growth trajectories that are responsible for adult morphology. We tested whether the close resemblance between *Tomistoma* and *Gavialis* may be produced by evolutionary convergence, as the morphological phylogeny proposes, or whether this similarity is derived from shared ontogeny (homology), as the molecular data suggests. Adult phenotypes (the raw material in systematics), are the result of complex developmental programs. How much species actually share their ontogenies depends in part on their phylogenetic relatedness, and on several interrelated processes, including selection, shared evolutionary history, and developmental "constraints."

When the direction of ontogenetic trajectories were examined, we found that *Tomistoma* possesses a unique direction and rate of growth in comparison to the other taxa. For the entire skull and for the rostrum, this difference is always significant, while for the postrostrum, *Tomistoma* differed significantly only from *Crocodylus*. These findings suggest that *Tomistoma* evolved a unique rate and trajectory of growth.

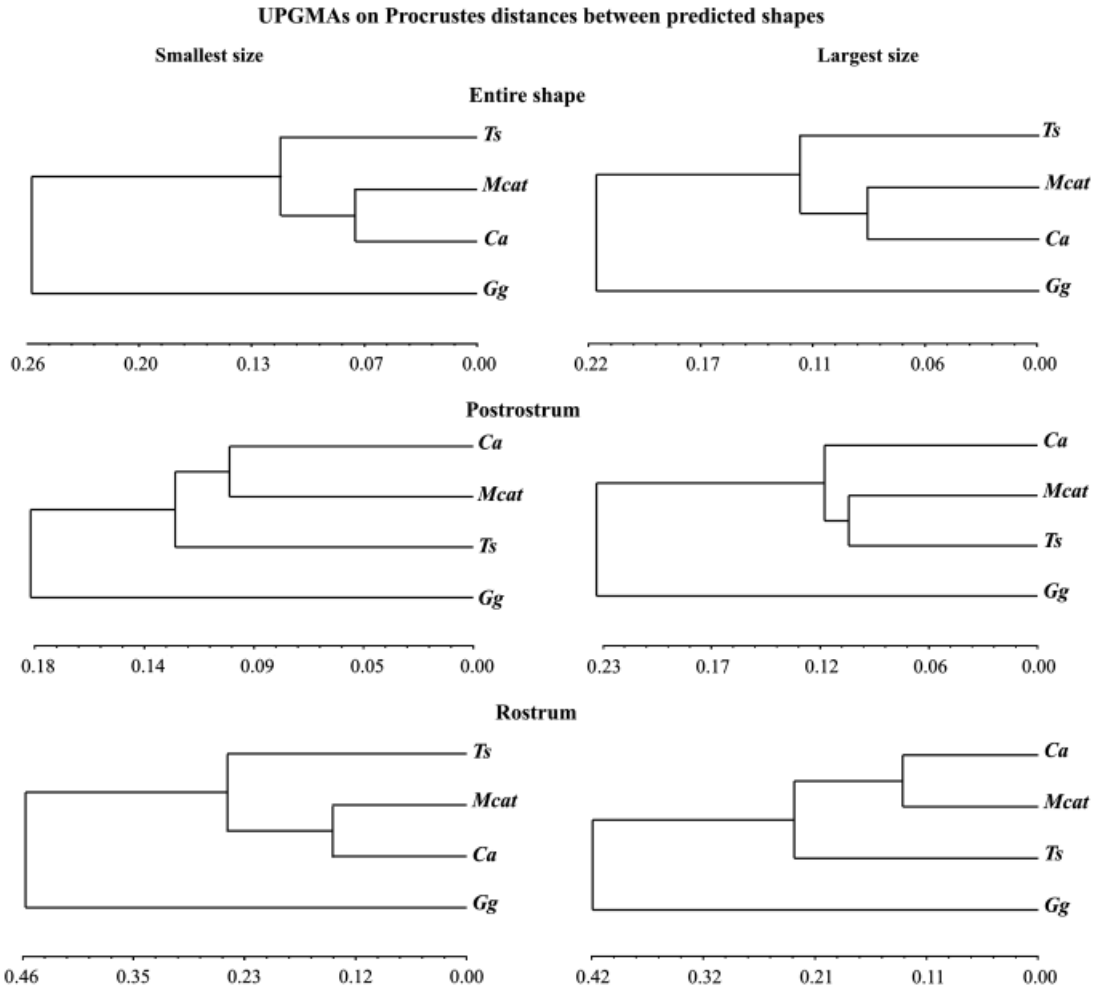

Fig. 6. UPGMA dendrograms performed on predicted shapes at small and large sizes for the three landmark data sets. *Ca*, *Crocodylus acutus*; *Mcat*, *Mecistops cataphractus*; *Gg*, *Gavialis gangeticus*; *Ts*, *Tomistoma schlegelii*.

On the other hand, looking at early developmental stages differences, *Tomistoma* is more similar to *Crocodylus* and *Mecistops*, while it appears clear that *Gavialis* "starts" its posthatching morphology from a completely different region of morphospace. This suggests that *Gavialis* possesses a drastically different morphology even at the onset of posthatching growth (Table 3, Fig. 6). Toward the end of development, *Gavialis* is found outside the group containing the other taxa, providing evidence consistent with the morphological and paleontological phylogeny. In fact, 3D representations of trajectories show that the trajectories of *Tomistoma*, *Mecistops*, and *Crocodylus* start in a common space region, while the *Gavialis* trajectory is unique from those of the other three taxa.

Together, the differences in the direction of ontogenetic trajectories and differences in skull shapes at small sizes, explain different features about similarities in morphogenesis. Differences in the slopes of ontogenetic trajectories represent different rates of morphological change relative to size, while differences in skull shape at small sizes represent differences in morphospace occupation at the onset of growth and development. While identifying differences in ontogenetic trajectories is straightforward, it is less clear is whether these differences represent a change in the developmental pathways underlying growth, or whether they represent important changes in gene expression and regulation (Burke et al. 1995).

Our results also reveal that the phenotypic resemblance between false and true gharial skulls is not due to convergence, nor to similar ontogenetic pathways. In fact, when ontogenetic process is studied in detail, the evident similarities occurring at adult stages, that is the longirostral shape, appear to be the result of morphological adaptation to a reduction of maximum prey size whose extreme condition is the strictly piscivorous diet of *Gavialis*. Sadleyr and Makovicky (2008) found that specific qualitative characters, used for cladistic analyses, are correlated with particular snout categories a

priori *defined*. However, rostral variation is continuously distributed in Crocodylia (Piras et al. 2009) and a GM analysis is capable of capturing the complexity of this pattern. As hypothesized by Sadleyr and Makovicky (2008), differences in ontogenetic trajectories reveal possible atavism or convergence/parallelism that underlies adult snout similarity. Further, even if one assumes that *Gavialis* and *Tomistoma* are sister taxa (as is found based on molecular data), this would not necessarily indicate that the long, slender snout was inherited from their last common ancestor. Such an inference would depend on where fossils were placed relative to extant taxa in the molecular phylogeny. For instance, if the primitive tomistomines *Maroccosuchus* and *Kentisuchus* (from Early Eocene of Morocco and England respectively, about 50 Ma) were closer to *Tomistoma* than to *Gavialis*, this placement would infer that a slender (stenorostrine) snout was the ancestral condition in the *Tomistoma*/*Gavialis* clade, while a truly long (longirostrine) snout might not be. However, this scenario ignores the placement of all fossil Gavialoidea that, from their oldest representatives (*Eothoracosaurus mississippiensis*, from Late Cretaceous of North America, about 70 Ma) showed an extreme longirostral condition.

When computing allometric trajectories of the four taxa separately we found much smaller covariation between shape and size in *Gavialis* rostrum than in *Tomistoma*'s: a further indication that the growth patterns of the two species for this module are quite different, and that *Gavialis* skull has a distinct growth pattern. On the other hand, *Gavialis* displays large covariation between postrostrum shape and size. Thus, comparing these patterns between taxa suggests that the two are quite distinct from a developmental point of view. Based on the results presented here, the distinct ontogenetic trajectories, as well as the distinct juvenile shapes, provide evidence that gharial shapes are distinct, and that there remains a close similarity between *Tomistoma* and the other brevirostres, supporting the morphological phylogenetic hypothesis.

CONCLUSIONS

Morphological and molecular approaches to crocodile phylogeny point to very different tree topologies. The morphological topology proposes that the Schlegel's crocodile, *T. schlegelii*, is closer to brevirostrine forms than to gharials, despite its long and slender rostrum and general morphological similarity to the latter. Here we argue that the longirostrine condition in *Tomistoma* and *Gavialis* is due to adaptive parallelism, probably generated by the very similar feeding habits of these species. Despite being longirostrine in skull shape, *Tomistoma*'s ontogenetic trajectories computed for both the skull as a whole and for its prominent modules (the rostrum and the postrostrum) are all much more similar to brevirostres' than to *Gavialis*. True gharial skull ontogeny is very unique. While the aberrant ontogeny of *G. gangeticus* makes its phylogenetic position problematic with the molecular approach, a close resemblance between *Tomistoma* and the other brevirostres is clearly supported.

Acknowledgments

We are very grateful to Michael Collyer for its important contributions on some statistical tests used in this paper. Paolo Piras had access to the collections of the Natural History Museum in London, the Institut Royal des Sciences Naturelles in Brussels and the Museum d'Histoire Naturelle in Paris thanks to the SYNTHESYS program, and to the collection of the Field Museum in Chicago thanks to the Visiting Scholarship Program. DCA was supported in part by NSF grant DEB-0446758.

REFERENCES

Adams, D. C. 2010. Paralell evolution of character displacement driven by competitive selection in terrestrial salamanders. *BMC Evol. Biol.* 10(72): 1–10.

Adams, D. C., and Collyer, M. L. 2007. Analysis of character divergence along environmental gradients and other covariates. *Evolution* 61: 510–515.

Adams, D. C., and Collyer, M. L. 2009. A general framework for the analysis of phenotypic change in evolutionary studies. *Evolution* 63: 1143–1154.

Adams, D. C., and Nistri, A. 2010. Ontogenetic convergence and evolution of foot morphology in European cave salamanders (Family: Plethodontidae). *BMC Evol. Biol.* 10(216): 1–10.

Adams, D. C., Rohlf, F. J., and Slice, D. E. 2004. Geometric morphometrics: ten years of progress following the 'revolution'. *It. J. Zool.* 71: 5–16.

Anderson, M. J. 2001. A new method for non-parametric multivariate analysis of variance. *Aust. Ecol.* 26: 32–46.

Bookstein, F. L. 1986. Size and shape spaces for landmark data in two dimensions. *Stat. Sci.* 1: 181–222.

Bookstein, E. L. 1991. *Morphometric tools for Landmark data: Geometry and Biology*. Cambridge University Press, New York.

Brochu, C. A. 2001. Crocodylian snouts in space and time: phylogenetic approaches toward adaptive radiation. *Am. Zool.* 41: 564–585.

Brochu, C. A. 2003. Phylogenetic approaches toward crocodylian history. *Ann. Rev. E. Plan. Sci.* 31: 357–397.

Brochu, C. A., and Densmore, L. D. 2001. Crocodile phylogenetics: a review of current progress. In G. Grigg, F. Seebacher, and C. E. Franklin (eds.). *Crocodilian Biology and Evolution*. Surrey Beatty & Sons New South Wales, Australia, pp. 3–8.

Burke, A. C., Nelson, C. E., Morgan, B. A., and Tabin, C. 1995. Hox genes and the evolution of vertebrate axial morphology. *Development* 121: 333–346.

Busbey, A. B. 1995. The structural consequences of skull flattening in crocodilians. In J. J. Thomason (ed.). *Functional Morphology in Vertebrate Paleontology*. Cambridge University Press, New York, pp. 173–192.

Collyer, M. L., and Adams, D. C. 2007. Analysis of two-state multivariate phenotypic change in ecological studies. *Ecology* 88: 683–692.

Gatesy, J., Amato, G., Norell, M., De Salle, R., and Hayashi, C. 2003. Total evidence support for extreme taxic atavism in gavialine crocodilians. *Syst. Biol.* 52: 403–422.

Gatesy, J., Baker, R. H., and Hayashi, C. 2004. Inconsistencies in arguments for the supertree approach: supermatrices versus supertrees of crocodylia. *Syst. Biol.* 53: 342–355.

Goodall, C. R. 1991. Procrustes methods in the statistical analysis of shape. *J. R. Stat. Soc. B* 53: 285–339.

Harshman, J., Huddleston, C., Bollback, J., Parsons, T., and Braun, M. 2003. True and false gharials: a nuclear gene phylogeny of crocodylia. *Syst. Biol.* 52: 386–402.

Janke, A., Gullberg, A., Hughes, S., Aggarwal, R. K., and Arnason, U. 2006. Mitogenomic analyses place the gharial (*Gavialis gangeticus*) on the crocodile tree and provide pre-K/T divergence times for most crocodilians. *J. Mol. Evol.* 61: 620–626.

McAliley, L. R., Willis, R. E., Ray, D. A., Scott White, P., Brochu, C. A., and Densmore, L. D. III 2006. Are crocodiles really monophyletic? Evidence for subdivisions from sequence and morphological data. *Mol. Phylogenet. Evol.* 39: 16–32.

Mitteroecker, P., and Bookstein, F. L. 2005. Heterochrony and geometric morphometrics: a comparison of cranial growth in *Pan paniscus* versus *Pan troglodytes*. *Evol. Dev.* 7: 244–258.

Mitteroecker, P., and Bookstein, F. L. 2008. The evolutionary role of modularity and integration in the hominoid cranium. *Evolution* 62: 943–958.

Mitteroecker, P., and Gunz, P. 2009. Advances in geometric morphometrics. *Evol. Biol.* 36: 235–247.

Mitteroecker, P., Gunz, P., Bernhard, M., Schaefer, K., and Bookstein, F. L. 2004. Comparison of cranialontogenetic trajectories among hominoids. *J. Hum. Evol.* 46: 679–698.

Piras, P., Teresi, L., Buscalioni, A. D. G., and Cubo, J. 2009. The shadow of forgotten ancestors differently constrains the fate of alligatoroidea and crocodyloidea. *Glob. Ecol. Biogeogr.* 18: 30–40.

Rohlf, F. J., and Marcus, L. F. 1993. A revolution in morphometrics. *Trends Ecol. Evol.* 8: 129–132.

Rohlf, F. J., and Slice, D. E. 1990. Extensions of the procrustes method for the optimal superimposition of landmarks. *Syst. Zool.* 39: 40–59.

Sadleyr, R. W., and Makovicky, P. J. 2008. Cranial shape and correlated characters in crocodilian evolution. *J. Evol. Biol.* 21: 1578–1596.

Xue-Feng, J., Xiao-Bing, W., Yan, L., Peng, Y., and Amato, G. 2006. The mitochondrial genome of *Crocodylus niloticus* with implications for phylogenetic relationships among crocodilian species. *Acta Zool. Sin.* 52: 810–818.

Zelditch, M. L., Swiderski, D. L., Sheets, H. D., and Fink, W. L. 2004. *Geometric Morphometrics for Biologists: A Primer*. Elsevier Academic Press, New York and London.

SUPPORTING INFORMATION

Additional Supporting Information may be found in the online version of this article:

Appendix S1. Material used for this study.

Please note: Wiley-Blackwell are not responsible for the content or functionality of any supporting materials supplied by the authors. Any queries (other than missing material) should be directed to the corresponding author for the article.